

Combined Fluorescence Spectroscopy and Molecular Docking Studies on the Interaction between 2,4-Dinitrophenyl Hydrazine-Derived Schiff Base and Bovine Serum Albumin

Tapan K. Rana ¹, Patitapaban Mohanty ², Pragyan P. Dash ², Priyaranjan Mohapatra ², Aruna K. Barick ², Pradip K. Jena ³, Lingaraj Behera ^{1,*}, Bigyan R. Jali ^{2,*}

¹ Department of Chemistry, Maharaja SriRam Chandra Bhanja Deo University, Baripada, Mayurbhanj, Odisha, India

² Department of Chemistry, Veer Surendra Sai University of Technology, Burla, Sambalpur 768018, Odisha, India

³ College of Basic Science and Humanities, OUAT, Bhubaneswar 751003, Odisha, India

* Correspondence: bigyan.Jali7@gmail.com (B.R.J.); lrbehera@yahoo.com (L.B.);

Received: 22.12.2023; Accepted: 30.06.2024; Published: 20.12.2025

Abstract: Proteins are the most abundant macromolecules in cells and are essential for maintaining normal cell activities. One of the most important components of plasma proteins is bovine serum albumin (BSA), which transports and metabolizes many endogenous and foreign chemicals. A novel and cost-effective Schiff base, derived from 2,4-dinitrophenyl hydrazine (L), was designed and synthesized. The synthesized molecular probe (L) was characterized using various spectroscopic techniques. The interaction between BSA and L was characterized using UV-Vis, fluorescence, dynamic light scattering (DLS), scanning electron microscopy (SEM), and differential scanning calorimetry (DSC). In phosphate buffer solution (pH = 7.4), BSA showed fluorescence maxima at 342 nm. Quenching fluorescence was observed upon incremental addition of L. The quenching of the fluorescence emission is due to the formation of a complex between BSA and L. The binding interaction was calculated from fluorescence titration and found to be 7.257×10^8 M. A molecular docking experiment was performed to establish the interaction between BSA and L.

Keywords: BSA; molecular probe; fluorescence; binding; UV-vis; docking; DFT-TD-DFT.

© 2025 by the authors. This article is an open-access article distributed under the terms and conditions of the Creative Commons Attribution (CC BY) license (<https://creativecommons.org/licenses/by/4.0/>), which permits unrestricted use, distribution, and reproduction in any medium, provided the original work is properly cited. The authors retain copyright of their work, and no permission is required from the authors or the publisher to reuse or distribute this article, as long as proper attribution is given to the original source.

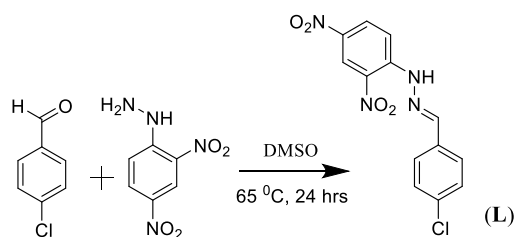
1. Introduction

The most common protein in blood is serum albumin, which is the main element of blood plasma [1-2]. The 3D structure of Serum albumin consists of three similar domains (III, II, I), which are further separated into A and B sub-domains. Molecular forces like hydrogen bonds, interaction with electrostatic forces, and hydrophobic forces are situated on the various binding sites, contributing to serum albumin's binding properties [3-4]. It primarily functions in the blood as a carrier for chemicals such as steroids, fatty acids, thyroid hormones, and other exogenous and endogenous compounds [5-7]. The primary structure of BSA consists of 17 disulfide linkages, and free cysteine residues are present in 583 amino acid residues. The amino acids 6-105 are found in BSA subdomain IA, while amino acids 119-196 are found in subdomain IB [8-10]. Amino acids 197-291, 314-481 and 511-583 are included in subdomains IIA, IIB, IIIA, and IIIB, respectively. Trp-134 in subdomain IB and Trp-212 in subdomain IIA

are the two tryptophan residues in BSA that act as intrinsic fluorophores [11-13]. BSA is used as a standard for protein due to its ability to increase signal in assays and its affordability and ease of mass production. Advantages of using BSA include serving as a blocking reagent in immunoassays, serving as a nutrient source in microbial cultures, serving as a carrier protein for conjugates, and serving as a protein supplement in cell culture media [14-16]. Due to the binding of ligands, the structure of the albumin changes due to hydrophobic contacts of the chromophore within the protein interior [17-19]. A fluorophore(tryptophan) could be present in the domain where the quencher can penetrate. BSA, Trp-214 trapped in the hydrophobic loop, and Trp-134 exposed to a hydrophilic environment (subdomain IIA of serum albumin) [20-21].

In numerous fields, including the quantitative, natural, and chemical sciences, Schiff bases constitute a significant class of the most frequently used organic molecules [22-23]. Due to their wide range of biological actions, including antimicrobial, antibacterial, anticonvulsant, antitubercular, chemotherapeutic, antioxidant, and insecticidal properties, Schiff bases have gained greater popularity in the medical and commercial fields [23-25]. The interaction of the Schiff base ligand can be studied using various methods, such as fluorescence, electrochemical, atomic absorption, voltammetry, and atomic emission spectroscopy [26-29]. The fluorescence method is mostly used for its high specificity, low cost, high sensitivity, simple operation, and quick response at low concentrations [30-33]. In both fundamental studies and practical applications involving organic molecules, the photophysical characteristics of the excited-state intramolecular electron-transfer mechanism in fluorescence spectroscopy have attracted significant interest [34-36].

Herein, we designed and synthesized a 2,4-dinitrophenylhydrazine-based Schiff base to study its interaction with BSA (Scheme 1). 2,4-dinitrophenylhydrazine is an important reagent in analytical chemistry and is used for the qualitative analysis of carbonyl groups. This 2,4-dinitrophenylhydrazine-based optical sensor has attracted significant attention for its outstanding sensitivity and specificity, low detection limits, quick and simple manufacturing, low cost, and non-destructive properties. Due to the structural conjugation, catalytic characteristics, and inherent attributes, 2,4-Dinitrophenylhydrazine is sensitive and effective.



Scheme 1. (E)-1-(4-chlorobenzylidene)-2-(2,4-dinitrophenyl) hydrazine (L) used for protein interactions.

2. Materials and Methods

2.1. Materials and equipment.

All chemicals, such as 4-chlorobenzaldehyde, 2,4-dinitrophenyl hydrazine, DMSO, and BSA, were procured from Sigma-Aldrich and used without purification. The BSA stock solution was prepared by dissolving BSA in 10 mM phosphate buffer at pH 7. The stock solution was stored in the refrigerator (5° C) and used only for up to 3 days. ¹H NMR (TMS as internal standard) and ¹³C NMR were recorded on an Agilent Technologies, Inc., CA, USA,

400 MHz instrument using DMSO-d₆ as solvent. The UV-vis study was performed using a Toshihin 1900i LS-55 spectrofluorimeter over the wavelength range of 200-600 nm. The FTIR spectrum was recorded using a Bruker Alpha ECO-ATR instrument over a wide range of wavenumbers from 4000 to 400 cm⁻¹. The UV-Vis study was performed using a Toshihin 1900i LS-55 spectrofluorimeter over the wavelength range of 200-600 nm. The fluorescence spectra are recorded using a Perkin-Elmer fluorescence spectrophotometer with a slit width of 5.0 nm and with a scan speed of 1200 nm min⁻¹. The particle size and hydrodynamic diameter of BSA and its complex were measured using a Zetasizer device from Malvern Panalytical Ltd., Hyogo, Japan, model no. ZEN-3690. All the experiments are performed at ambient conditions. Doubly distilled, deionized water was used throughout the experiment where necessary.

2.2. Synthesis and characterization.

A hydrazine based Schiff based ligand (E)-1-(4-chlorobenzylidene)-2-(2,4-dinitrophenyl) hydrazine (**L**) was designed and prepared by the 1:1 addition of 2,4-dinitrophenyl hydrazine and 4-chlorobenzaldehyde in DMSO, as previously reported (Scheme S1). The solution was stirred at room temperature for 20 hours, and an orange-red precipitate was obtained, which was filtered. The orange-red color precipitate was allowed to dry in the open air. The ligand was characterized by various spectral analyses. ¹H NMR: (400 MHz, DMSO-d₆) δ 11.71 (s, 1H), 8.87 (d, J = 2.6 Hz, 1H), 8.71 (d, J = 5.1 Hz, 2H), 8.39 (dd, J = 9.6, 2.6 Hz, 1H), 8.12 (d, J = 9.6 Hz, 1H), 7.90 (d, J = 8.5 Hz, 1H), 7.83 (d, J = 8.5 Hz, 1H), 7.58 (t, J = 8.9 Hz, 2H); ¹³C NMR: (101 MHz, DMSO) δ 148.24, 144.63, 139.75, 136.62, 134.9, 130.22, 129.31, 129.18, 123.18 and 117.04. IR: (KBr, cm⁻¹): 3282 (W), 1601 (S), 1503 (S), 1322 (W), 1126 (S), 1079 (S), 819 (S), 609 (S). Mass (ESI) found m/z: 286.07; Calculated exact mass for C₁₃H₁₂N₂O₅; 245.0743.

2.3. Protein binding studies.

The interaction of BSA with the synthesized ligand **L** has been studied extensively using UV-visible and fluorescence spectroscopy. The BSA solution was prepared in phosphate buffer at pH 7, and the ligand solution was prepared in DMSO at a concentration of 10⁻⁴ M. The absorption study was carried out by adding the ligand incrementally to a fixed amount of BSA in Buffer. Further, the fluorescence quenching analysis (λ_{ex} = 290 nm) was performed by gradually incorporating the ligand into BSA in Buffer solution. The fluorescence quenching mechanism can be explained by the Stern-Volmer equation.

$$\frac{F_0}{F} = 1 + K_{sv}[Q] \dots(1)$$

In the above equation, the emission intensity in the absence and presence of the quencher was defined by F₀ and F, respectively. K_{sv} is the Stern-Volmer constant, and [Q] is the quencher concentration.

3. Results and Discussion

The molecular probe was designed based on previously reported procedures [37-38] and is shown in Scheme 1. The formation of the Schiff base and its structure were confirmed by analytical and spectroscopic techniques like ¹H NMR, ¹³C NMR, and FTIR (Figure S1-S3). The binding interaction of the Schiff base with BSA was further investigated using various photophysical analyses, including UV-visible and Fluorescence emission spectroscopy. The

changes in BSA and its surface morphology in the presence of L were also investigated using scanning electron microscopy (SEM) and dynamic light scattering (DLS).

3.1. Optimization of the geometry of L.

The stability analysis of the L follows a methodology comparable to that outlined earlier, and the resulting outcomes include data on the HOMO-LUMO energy gap, UV-Vis absorption spectra, and related parameters [39-43]. The optimized geometries of the ligand L within the gas and solvent (DMSO) medium are depicted in Figures 1a and 1b.

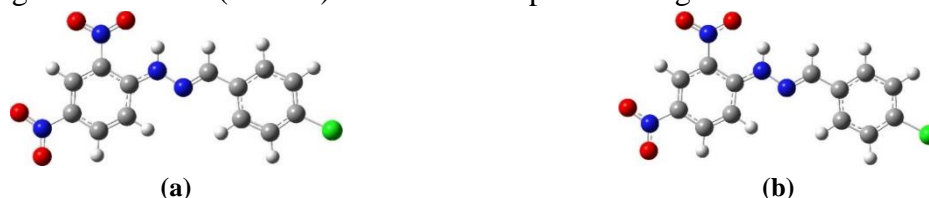


Figure 1. Optimized geometries of the ligand L (a) in gas phase; (b) in solvent (DMSO) medium.

For the ligand L, a notable reduction in the HOMO-LUMO energy gap was observed, enhancing the favorability of electronic transitions. Notably, among the entries in Table 1, this ligand exhibited the smallest energy gap in the solvent medium. These findings are substantiated by TD-DFT calculations, revealing the most preferred electronic transition at 423.09 nm for the L, as illustrated in Figures S3-S4.

Table 1. HOMO and LUMO Energy Gap of L.

	In the gas phase	In the solvent phase (DMSO)
HOMO		
LUMO		
E_h	-6.679	-6.394
E_l	-3.417	-3.323
ΔE	3.262	3.071

3.2. UV-Vis absorption spectra.

UV-Vis absorption analysis is a technique for examining the structural change and formation of a complex [44]. BSA exhibited absorption maxima at 276 nm. The absorption band at 276 nm appeared for BSA because of $\pi \rightarrow \pi^*$ transition (Figure S4).

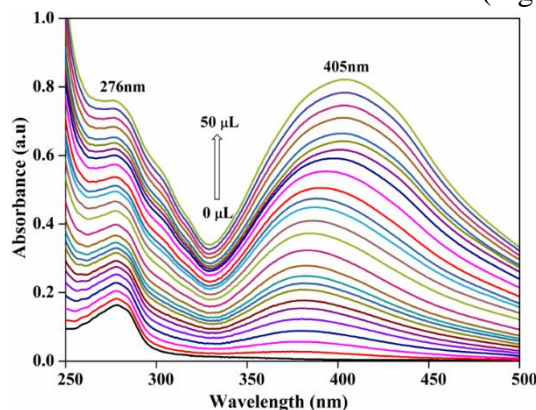


Figure 2. UV-Vis spectra of BSA (4 μ M, 3 mL, and phosphate buffer pH = 7.4) upon the addition of various concentrations of L in DMSO (10^{-6} M).

The addition of **L** to the BSA buffer solution causes a drastic shift in BSA's absorption band. The enhancement and raising of the new absorption band at a higher wavelength is due to the formation of a complex between BSA and **L** (Figure 2 and Figure S5). To find more information about the formation of complex, steady-state fluorescence emission, experiments have been carried out.

3.3. Fluorescence emission studies.

Fluorescence is a highly sensitive and precise technique for studying biological and other chemical systems. The BSA exhibited a strong emission peak at 342 nm when excited at 290 nm (Figure 3a). The tryptophan residue in BSA caused a fluorescence peak at 342 nm (Figure S6). In the presence of **L**, the quenched fluorescence of BSA was observed. With the gradual addition of **L**, the fluorescence intensity of BSA at 342 nm decreased, accompanied by a blue shift from 342 nm to 331 nm (Figure S7-S8). The alteration in fluorescence intensity and the blue shift in wavelength provide evidence for a stable hydrophobic interaction between BSA and **L**. It forms a stable complex between **L** and BSA. The Stern-Volmer equation 1 was utilized to investigate the quenching of BSA's fluorescence in more detail [45-46]. After doing the Stern-Volmer plot F_0/F vs $[Q]$, the result was 6.745×10^6 M (Figure 3b, Table 2). Additionally, the steady-state fluorescence anisotropy experiment has been conducted in the presence and absence of BSA to obtain more information on the formation of the complex [47].

Table 2. Stern-Volmer constant and anisotropy of BSA with **L**.

Complex ^a	K_{SV} (M) $\times 10^8$	Anisotropy of BSA ^b
BSA +L	7.257	0.164

a = 4 μ M BSA (3 mL) in 10mM in phosphate buffer, pH = 7.4; **b** = Anisotropy of BSA = 0.635.

Equation 1 has been used to calculate the fluorescence anisotropy of BSA in both the presence and absence of **L**. The anisotropy values rise from 0.635 to 0.164 (Table 2) when different concentrations of **L** are added to BSA, indicating that interactions between the probes and BSA occurred. Increased anisotropy values validated the shape change of the BSA protein [48].

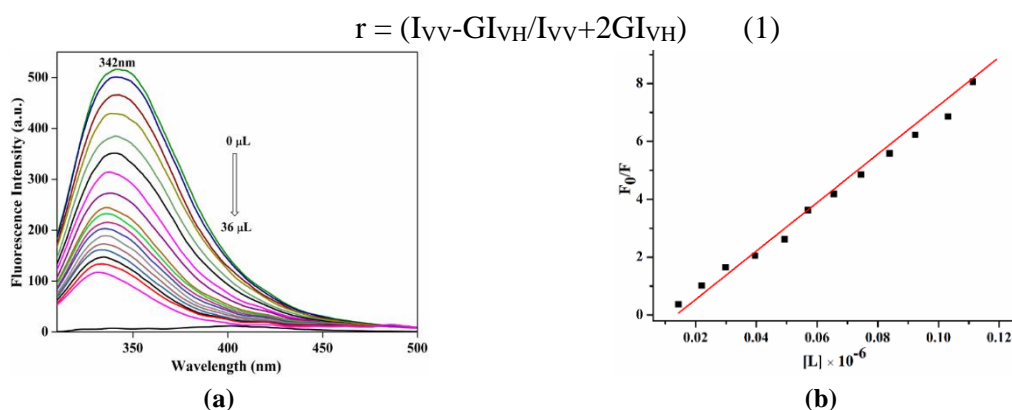


Figure 3. (a) Fluorescence spectral changes of BSA (4 μ M, 3 mL, and phosphate buffer pH = 7.4) upon the addition of various concentrations of **L** in DMSO (10^{-6} M); (b) Stern-Volmer plot.

3.4. DSC, DLS, and SEM studies.

To find additional evidence for the interaction between BSA and **L**, various analyses, including dynamic light scattering (DLS), scanning electron microscopy (SEM), and differential scanning calorimetry (DSC), are performed. The DLS technique is used to

investigate the physical characteristics of the complex in solution, including polydispersity, hydrodynamic diameter, and aggregation behavior. Figure 4a illustrates the size distribution curve of BSA and BSA-L complexes in a buffer solution. Upon the addition of ligand to BSA, the aggregation and size distribution of the system change due to the formation of a complex between BSA and ligand. The PDI value also changed from 0.738 to 0.480. The lower PDI value (less than 1) and the correlation coefficient plot (Figure S8) indicate the highly monodisperse nature of BSA, whether in the absence or presence of L. The formation of L aggregates was facilitated by an increase in particle size from 72.93 nm to 222.1 nm. It reveals that the BSA unfolds in the presence of L. The surface morphology of the BSA in the absence and presence of L is recorded using SEM analysis (Figure 4b). The ligand in DMSO has distinct needle-like crystals of small size. In the presence of BSA, the ligand's morphology changes, and the needle-shaped crystallinity of L is lost. The needle-shaped crystallinity of L changed to a bulk-shaped agglomerated crystal in the presence of BSA. The change in morphology of the L in the presence of BSA indicates the hydrophobic interaction between BSA and L. The DSC analysis of BSA in the absence and presence of L is also performed to analyze their phase transition temperature. It was also used to investigate the denaturation temperature of BSA in the presence and absence of L. The flat baseline in the DSC curve indicates their great purity (Figure 4c). The increase in the endothermic temperature may indicate a hydrophobic interaction between L and BSA.

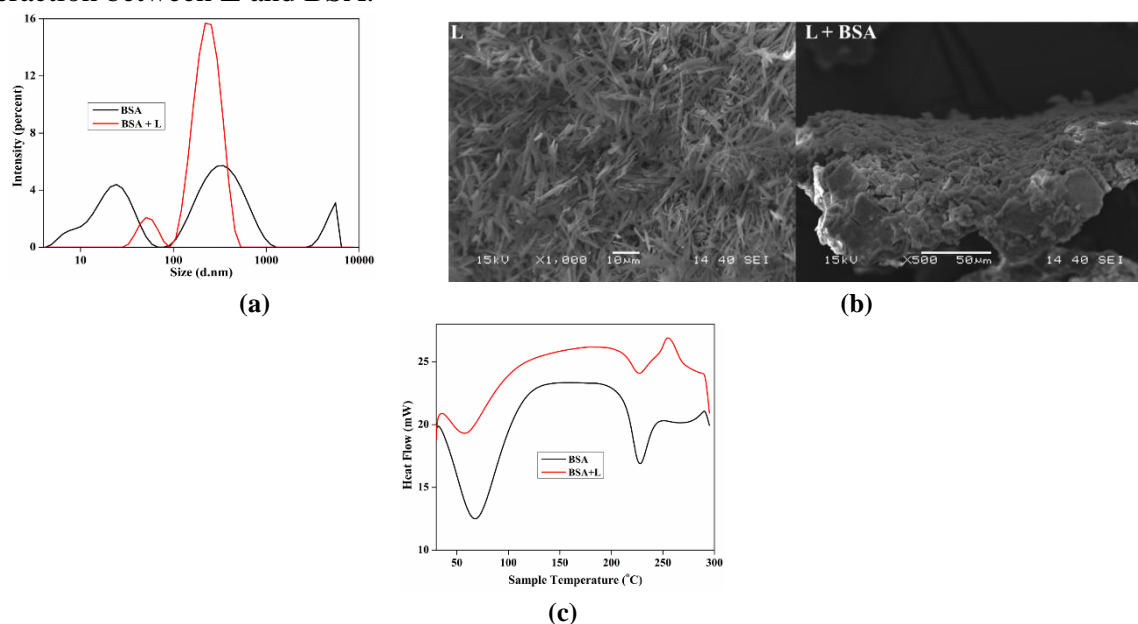


Figure 4. (a) DLS spectra of BSA and BSA + L complex; (b) SEM images of L and BSA + L complex; (c) DSC of BSA and BSA + L complex.

3.5. Molecular docking analysis.

A molecular docking analysis was performed to determine the interaction between L and the native protein [49]. The molecular probe L formed hydrogen bonds with Arg217 and Arg194 in BSA, while encountering three unfavorable interactions with Arg198, His241, and Arg217. These interactions resulted in an interaction energy of -8.8 kcal/mol (Figure 5). The interaction of various amino acid residues of BSA with L is shown in Table 3.

Funding

This research was funded by DST-Biotechnology, Govt. of Odisha, and Project No.: ST-BT-MISC-0008-2020-245/ST, dated 12-01-2022 and EEQ/2023/000069, Govt. of India.

Acknowledgments

Dr. Jali thanks DST-Biotechnology, Govt. of Odisha and Project No.: ST-BT-MISC-0008-2020-245/ST, dated 12-01-2022 and EEQ/2023/000069, Govt. of India. The authors also thank the Department of Chemistry, VSSUT, Burla, for providing a research facility.

Conflicts of Interest

The authors declare no conflict of interest.

Reference

1. Chen, Y.; Li, K.; Zhang, S.; Xu, P.; Song, B. Turn-on fluorescence probe for BSA detection and selective cell imaging. *Dyes Pigm.* **2022**, *202*, 110267, <https://doi.org/10.1016/j.dyepig.2022.110267>.
2. Jana, G.C.; Nayim, S.; Sahoo, N.K.; Das, S.; Aktara, M.N.; Patra, A.; Islam, M.M.; Hossain, M. Deciphering the positional impact of chlorine in a new series of berberine analogues towards the superb-selective “turn-on” hydrophobic signaling of bovine serum albumin at physiological pH. *New J. Chem.* **2020**, *44*, 1761-1771, <https://doi.org/10.1039/C9NJ05642D>.
3. Gomes, V.S.D.; Gonçalves, H.M.R.; Boto, R.E.F.; Almeida, P.; Reis, L.V. Barbiturate squaraine dyes as fluorescent probes for serum albumins detection. *J. Photochem. Photobiol. A Chem.* **2020**, *400*, 112710, <https://doi.org/10.1016/j.jphotochem.2020.112710>.
4. Szymaszek, P.; Fiedor, P.; Chachaj-Brekiesz, A.; Tyszka-Czochara, M.; Świergosz, T.; Ortyl, J. Molecular interactions of bovine serum albumin (BSA) with pyridine derivatives as candidates for non-covalent protein probes: aspectroscopic investigation. *J. Mol. Liq.* **2022**, *347*, 118262, <https://doi.org/10.1016/j.molliq.2021.118262>.
5. Behera, S.; Dash, P.P.; Bishoyi, A.K.; Dash, K.; Mohanty, P.; Sahoo, C.R.; Padhy, R.N.; Mishra, M.; Ghosh, B.N.; Sahoo, H.; Jali, B.R. Protein interactions, molecular docking, antimicrobial and antifungal studies of terpyridine ligands. *J. Biomol. Struct. Dyn.* **2022**, *41*, 11274-11285, <https://doi.org/10.1080/07391102.2022.2161012>.
6. Jali, B.R.; Kuang, Y.; Neamati, N.; Baruah, J.B. Selective binding of naphthoquinone derivatives to serum albumin proteins and their effects on cytotoxicity. *Chem.-Biol. Interact.* **2014**, *214*, 10-17, doi: 10.1016/j.cbi.2014.01.014..
7. Ghosh, K.; Rathi, S.; Arora, D. Fluorescence spectral studies on interaction of fluorescent probes with Bovine Serum Albumin (BSA). *J. Lumin.* **2016**, *175*, 135-140, <https://doi.org/10.1016/j.jlumin.2016.01.029>.
8. Mandal, B.; Chowdhury, N.; Baildya, N.; Mandal, R.P.; Bagchi, A.; De, S. Fluorescence probing and molecular docking analysis of the binding interaction of bovine serum albumin (BSA) with the polarity probe AICCN. *Phys. Chem. Chem. Phys.* **2023**, *25*, 18197-18214, <https://doi.org/10.1039/D2CP04124C>.
9. Kompany-Zareh, M.; Akbarian, S.; Najafpour, M.M. Unsupervised recognition of components from the interaction of BSA with Fe cluster in different conditions utilizing 2D fluorescence spectroscopy. *Sci. Rep.* **2022**, *12*, 16875, <https://doi.org/10.1038/s41598-022-20768-6>.
10. Behera, S.; Behura, R.; Mohanty, P.; Sahoo, M.; Subrahmanya, R.D.; Verma, A.K.; Jali, B.R. Study of Interaction Between Bovine Serum Albumin and Dolutegravir Intermediate: Fluorescence and Molecular Docking Analysis. *Biointerface Res. Appl. Chem.* **2021**, *11*, 13102-13110, <https://doi.org/10.33263/BRIAC115.1310213110>.
11. Mulla, K.; Morin, J.-F. Probing the Interactions Between Anthanthrene Derivatives and Bovine Serum Albumin (BSA) Through Aggregation Induced Emission. *ChemistrySelect.* **2023**, *8*, e202300611, <https://doi.org/10.1002/slct.202300611>.
12. Bhui, S.; Halder, S.; Saha, S.K.; Chakravarty, M. Binding interactions and FRET between bovine serum albumin and various phenothiazine-/anthracene-based dyes: a structure-property relationship. *RSC Adv.* **2021**, *11*, 1679-1693, <https://doi.org/10.1039/D0RA09580J>.

13. El Gammal, R.N.; Elmansi, H.; EI-Emam, A.A.; Belal, F.; Hammouda, M.E.A. Exploring the molecular interaction of mebendazole with bovine serum albumin using multi-spectroscopic approaches and molecular docking. *Sci. Rep.* **2022**, *12*, 11582, <https://doi.org/10.1038/s41598-022-15696-4>.
14. Wei, J.; Xu, D.; Zhang, X.; Yang, J.; Wang, Q. Evaluation of anthocyanins in *Aronia melanocarpa*/BSA binding by spectroscopic studies. *AMB Expr.* **2018**, *8*, 72, <https://doi.org/10.1186/s13568-018-0604-5>.
15. Behera, S.; Mohanty, P.; Dash, P.P.; Mohapatra, P.; Shubhadarshinee, L.; Behura, R.; Barick, A.K.; Mohapatra, P.; Jali, B.R. Selective Binding of Bovine Serum Albumin (BSA): A Comprehensive Review. *Biointerface Res. Appl. Chem.* **2023**, *13*, 555, <https://doi.org/10.33263/BRIAC136.555>.
16. Moradi, Z.; Khorasani-Motlagh, M.; Rezvani, A.R.; Noroozifar, M. Electronic and fluorescent studies on the interaction of DNA and BSA with a new ternary praseodymium complex containing 2,9-dimethyl 1,10-phenanthroline and antibacterial activities testing. *J. Biomol. Struct. Dyn.* **2019**, *37*, 2283-2295, <https://doi.org/10.1080/07391102.2018.1479657>.
17. Behera, S.; Dash, P.P.; Mohanty, P.; Behura, R.; Sahoo, S.K.; Jali, B.R. Water-induced fluorescence turn-on imidazole derivative and its interaction with bovine serum albumin. *J. Mol. Struct.* **2023**, *1282*, 135158, <https://doi.org/10.1016/j.molstruc.2023.135158>.
18. Lee, S.-J.; Cho, H.-G.; Cheong, B.-S. Interaction of Bovine Serum Albumin with Propyl Gallate and Methyl Gallate Investigated by Fluorescence Spectroscopy. *Bull. Korean Chem. Soc.* **2019**, *40*, 344-351, <https://doi.org/10.1002/bkcs.11688>.
19. Shi, X.; Li, D.; Xie, J.; Wang, S.; Wu, Z.Q.; Chen, H. Spectroscopic investigation of the interactions between gold nanoparticles and bovine serum albumin. *Chin. Sci. Bull.* **2012**, *57*, 1109-1115, <https://doi.org/10.1007/s11434-011-4741-3>.
20. Jali, B.R. Investigation on bindings of a binaphthoquinone derivative with serum albumin proteins by fluorescence spectroscopy. *Indian J. Chem. A* **2021**, *60A*, 824-829, <https://doi.org/10.56042/ijca.v60i6.43630>.
21. Bhattacharya, B.; Nakka, S.; Guruprasad, L.; Samanta, A. Interaction of Bovine Serum Albumin with Dipolar Molecules: Fluorescence and Molecular Docking Studies. *J. Phys. Chem. B* **2009**, *113*, 2143-2150, <https://doi.org/10.1021/jp808611b>.
22. Dhanshi, S.; Dutta, S.; Sahoo, S.K. A Schiff base fluorescence switch-on probe derived from vitamin B₆ cofactor for simultaneous detection of bovine serum albumin and ovalbumin. *J. Photochem. Photobiol. A Chem.* **2023**, *444*, 114905, <https://doi.org/10.1016/j.jphotochem.2023.114905>.
23. Mohanty, P.; Behura, R.; Bhardwaj, V.; Dash, P.P.; Sahoo, S.K.; Jali, B.R. Recent advancement on chromo-fluorogenic sensing of aluminum (III) with Schiff bases. *Trends Environ. Anal. Chem.* **2022**, *34*, e00166, <https://doi.org/10.1016/j.teac.2022.e00166>.
24. Dash, P.P.; Patel, D.A.; Mohanty, P.; Behura, R.; Behera, S.; Sahoo, S.K.; Jali, B.R. Advances on chromo-fluorogenic sensing of copper (II) with Schiff bases. *Inorganica Chim. Acta* **2023**, *556*, 121635, <https://doi.org/10.1016/j.ica.2023.121635>.
25. Behera, S.; Behura, R.; Mohanty, M.; Dinda, R.; Mohanty, P.; Verma, A.K.; Sahoo, S.K.; Jali, B.R. Spectroscopic, cytotoxicity and molecular docking studies on the interaction between 2,4-dinitrophenylhydrazine derived Schiff bases with bovine serum albumin. *Sens. Int.* **2020**, *1*, 100048, <https://doi.org/10.1016/j.sintl.2020.100048>.
26. Rodríguez, M.; Ramos-Ortíz, G.; Maldonado, J.L.; Herrera-Ambriz, V.M.; Domínguez, O.; Santillan, R.; Farfán, N.; Nakatani, K. Structural, thermal and optical characterization of a Schiff base as a new organic material for nonlinear optical crystals and films with reversible noncentrosymmetry. *Spectrochim. Acta A Mol. Biomol. Spectrosc.* **2011**, *79*, 1757-1761, <https://doi.org/10.1016/j.saa.2011.05.051>.
27. Behura, R.; Mohanty, P.; Sahu, G.; Dash, P.P.; Behera, S.; Dinda, R.; Hota, P.R.; Sahoo, H.; Bhaskaran, R.; Barick, A.K.; Mohapatra, P.; Jali, B.R. A highly selective Schiff base fluorescent sensor for Zn²⁺, Cd²⁺ and Hg²⁺ based on 2,4-dinitrophenylhydrazine derivative. *Inorg. Chem. Commun.* **2023**, *154*, 110959, <https://doi.org/10.1016/j.inoche.2023.110959>.
28. Yan, F.; Fan, K.; Ma, T.; Xu, J.; Wang, J.; Ma, C. Synthesis and spectral analysis of fluorescent probes for Ce⁴⁺ and OCl⁻ ions based on fluorescein Schiff base with amino or hydrazine structure: Application in actual water samples and biological imaging. *Spectrochim. Acta A Mol. Biomol. Spectrosc.* **2019**, *213*, 254-262, <https://doi.org/10.1016/j.saa.2019.01.045>.
29. Tian, F.-F.; Jiang, F.-L.; Han, X.-L.; Xiang, C.; Ge, Y.-S.; Li, J.-H.; Zhang, Y.; Li, R.; Ding, X.-L.; Liu, Y. Synthesis of a Novel Hydrazone Derivative and Biophysical Studies of Its Interactions with Bovine Serum

- Albumin by Spectroscopic, Electrochemical, and Molecular Docking Methods. *J. Phys. Chem. B* **2010**, *114*, 14842-14853, <https://doi.org/10.1021/jp105766n>.
30. Kaur, N.; Chopra, S.; Singh, G.; Raj, P.; Bhasin, A.; Sahoo, S.K.; Kuwar, A.; Singh, N. Chemosensors for biogenic amines and biothiols. *J. Mater. Chem. B* **2018**, *6*, 4872-4902, <https://doi.org/10.1039/C8TB00732B>.
 31. Dash, P.P.; Mohanty, P.; Behura, R.; Behera, S.; Singla, P.; Sahoo, S.C.; Sahoo, S.K.; Jali, B.R. Detection of moisture in DMSO and raw food products by using an anthracene-based fluorescence OFF-ON chemosensor. *J. Photochem. Photobiol. A Chem.* **2023**, *440*, 114650, <https://doi.org/10.1016/j.jphotochem.2023.114650>.
 32. Dash, P.P.; Mohanty, P.; Behura, R.; Behera, S.; Naik, S.; Mishra, M.; Sahoo, H.; Barick, A.K.; Mohapatra, P.; Sahoo, S.K.; Jali, B.R. Rapid Colorimetric and Fluorometric Discrimination of Maleic Acid vs. Fumaric Acid and Detection of Maleic Acid in Food Additives. *J. Fluoresc.* **2024**, *34*, 1015-1024, <https://doi.org/10.1007/s10895-023-03330-z>.
 33. Bhowmik, S.; Ghosh, B.N.; Marjomäki, V.; Rissanen, K. Nanomolar Pyrophosphate Detection in Water and in a Self-Assembled Hydrogel of a Simple Terpyridine-Zn²⁺ Complex. *J. Am. Chem. Soc.* **2014**, *136*, 5543-5546, <https://doi.org/10.1021/ja4128949>.
 34. Mohanty, P.; Dash, P.P.; Naik, S.; Behura, R.; Mishra, M.; Sahoo, H.; Sahoo, S.K.; Barick, A.K.; Jali, B.R. A thiourea-based fluorescent turn-on chemosensor for detecting Hg²⁺, Ag⁺ and Au³⁺ in aqueous medium. *J. Photochem. Photobiol. A Chem.* **2023**, *437*, 114491, <https://doi.org/10.1016/j.jphotochem.2022.114491>.
 35. Dash, P.P.; Mohanty, P.; Behera, S.; Behura, R.; Palai, B.B.; Nath, B.; Sahoo, S.K.; Jali, B.R. Pyrene-based fluorescent chemosensor for rapid detection of water and its applications. *Methods* **2023**, *219*, 127-138, <https://doi.org/10.1016/j.ymeth.2023.10.006>.
 36. Hamilton, G.R.C.; Sahoo, S.K.; Kamila, S.; Singh, N.; Kaur, N.; Hyland, B.W.; Callan, J.F. Optical probes for the detection of protons, and alkali and alkaline earth metal cations. *Chem. Soc. Rev.* **2015**, *44*, 4415-4432, <https://doi.org/10.1039/C4CS00365A>.
 37. Behura, R.; Dash, P.P.; Mohanty, P.; Behera, S.; Mohanty, M.; Dinda, R.; Behera, S.K.; Barick, A.K.; Jali, B.R. A Schiff base luminescent chemosensor for selective detection of Zn²⁺ in aqueous medium. *J. Mol. Struct.* **2022**, *1264*, 133310, <https://doi.org/10.1016/j.molstruc.2022.133310>.
 38. Behura, R.; Behera, S.; Mohanty, P.; Dash, P.P.; Panigrahi, R.; Mallik, B.S.; Sahoo, S.K.; Jali, B.R. Fluorescent sensing of water in DMSO by 2,4-dinitrophenyl hydrazine derived Schiff base. *J. Mol. Struct.* **2022**, *1251*, 132086, <https://doi.org/10.1016/j.molstruc.2021.132086>.
 39. Frisch, M.J.; Trucks, G.W.; Schlegel, H.B.; Scuseria, G.E.; Robb, M.A.; Cheeseman, J.R.; Scalmani, G.; Barone, V.; Mennucci, B.; Petersson, G.A.; Nakatsuji, H.; Caricato, M.; Li, X.; Hratchian, H.P.; Izmaylov, A.F.; Bloino, J.; Zheng, G.; Sonnenberg, J.L.; Hada, M.; Ehara, M.; Toyota, K.; Fukuda, R.; Hasegawa, J.; Ishida, M.; Nakajima, T.; Honda, Y.; Kitao, O.; Nakai, H.; Vreven, T.; Montgomery, Jr., J.A.; Peralta, J.E.; Ogliaro, F.; Bearpark, M.; Heyd, J.J.; Brothers, E.; Kudin, K.N.; Staroverov, V.N.; Kobayashi, R.; Normand, J.; Raghavachari, K.; Rendell, A.; Burant, J.C.; Iyengar, S.S.; Tomasi, J.; Cossi, M.; Rega, N.; Millam, J.M.; Klene, M.; Knox, J.E.; Cross, J.B.; Bakken, V.; Adamo, C.; Jaramillo, J.; Gomperts, R.; Stratmann, R.E.; Yazyev, O.; Austin, A.J.; Cammi, R.; Pomelli, C.; Ochterski, J.W.; Martin, R.L.; Morokuma, K.; Zakrzewski, V.G.; Voth, G.A.; Salvador, P.; Dannenberg, J.J.; Dapprich, S.; Daniels, A.D.; Farkas, Ö.; Å.; Foresman, J.B.; Ortiz, J.V.; Cioslowski, J.; Fox, D.J. Gaussian 09, Gaussian, Inc., Wallingford, CT, USA, **2009**.
 40. Cancès, E.; Mennucci, B.; Tomasi, J. A new integral equation formalism for the polarizable continuum model: Theoretical background and applications to isotropic and anisotropic dielectrics. *J. Chem. Phys.* **1997**, *107*, 3032-3041, <https://doi.org/10.1063/1.474659>.
 41. Miertuš, S.; Scrocco, E.; Tomasi, J. Electrostatic interaction of a solute with a continuum. A direct utilization of AB initio molecular potentials for the prevision of solvent effects. *Chem. Phys.* **1981**, *55*, 117-129, [https://doi.org/10.1016/0301-0104\(81\)85090-2](https://doi.org/10.1016/0301-0104(81)85090-2).
 42. Becke, A.D. Density- functional thermochemistry. III. The role of exact exchange. *J. Chem. Phys.* **1993**, *98*, 5648-5652, <https://doi.org/10.1063/1.464913>.
 43. Lee, C.; Yang, W.; Parr, R.G. Development of the Colle-Salvetti correlation-energy formula into a functional of the electron density. *Phys. Rev. B* **1988**, *37*, 785, <https://doi.org/10.1103/PhysRevB.37.785>.
 44. Buddanavar, A.T.; Nandibewoor, S.T. Multi-spectroscopic characterization of bovine serum albumin upon interaction with atomoxetine. *J. Pharm. Anal.* **2017**, *7*, 148-155, <https://doi.org/10.1016/j.jpha.2016.10.001>.

45. Lakowicz, J.R. Principles of Fluorescence Spectroscopy, 3rd Edition. Springer: New York, New York, **2013**; 25-698, <https://doi.org/10.1007/978-1-4757-3061-6>.
46. Rana, T. K., Mohanty, P., Dash, P. P., Mohapatra, P., Barick, A. K., Jena, P.K., Bejara, L., Jali, B. R Protein Interaction and Molecular Docking Analysis by Schiff Base Derived from 2,4-Dinitro Phenyl Hydrazine. *J. Mol. Eng. Mater* **2024**, *12*, 2450008. <https://doi.org/10.1142/S2251237324500084>.
47. González Flecha, F.L.; Levi, V. Determination of the molecular size of BSA by fluorescence anisotropy. *Biochem. Mol. Biol. Educ.* **2003**, *31*, 319-322, <https://doi.org/10.1002/bmb.2003.494031050261>.
48. Rana, T. K., Mohanty, P., Dash, P. P., Mishra, S., Tripathi, S. S., Mohapatra, P., Barick, A. K., Jena, P.K., Bhaskaran, R., Khan, M. S., Khan, M. R., Behera, L., Jali, B. R., Unveiling Fluorescence Spectroscopy, Molecular Docking and Dynamic Simulations: Interactions Between Protein and 2, 4-Dinitrophenylhydrazine Schiff Base. *J Fluoresc* **2025**, *35*, 6127–6136. <https://doi.org/10.1007/s10895-024-03939-8>.
49. Nnyigide, O.S.; Lee, S.-G.; Hyun, K In Silico Characterization of the Binding Modes of Surfactants with Bovine Serum Albumin. *Sci. Rep.* **2019**, *9*, 10643, <https://doi.org/10.1038/s41598-019-47135-2>.

Publisher’s Note & Disclaimer

The statements, opinions, and data presented in this publication are solely those of the individual author(s) and contributor(s) and do not necessarily reflect the views of the publisher and/or the editor(s). The publisher and/or the editor(s) disclaim any responsibility for the accuracy, completeness, or reliability of the content. Neither the publisher nor the editor(s) assume any legal liability for any errors, omissions, or consequences arising from the use of the information presented in this publication. Furthermore, the publisher and/or the editor(s) disclaim any liability for any injury, damage, or loss to persons or property that may result from the use of any ideas, methods, instructions, or products mentioned in the content. Readers are encouraged to independently verify any information before relying on it, and the publisher assumes no responsibility for any consequences arising from the use of materials contained in this publication.

Supplementary materials

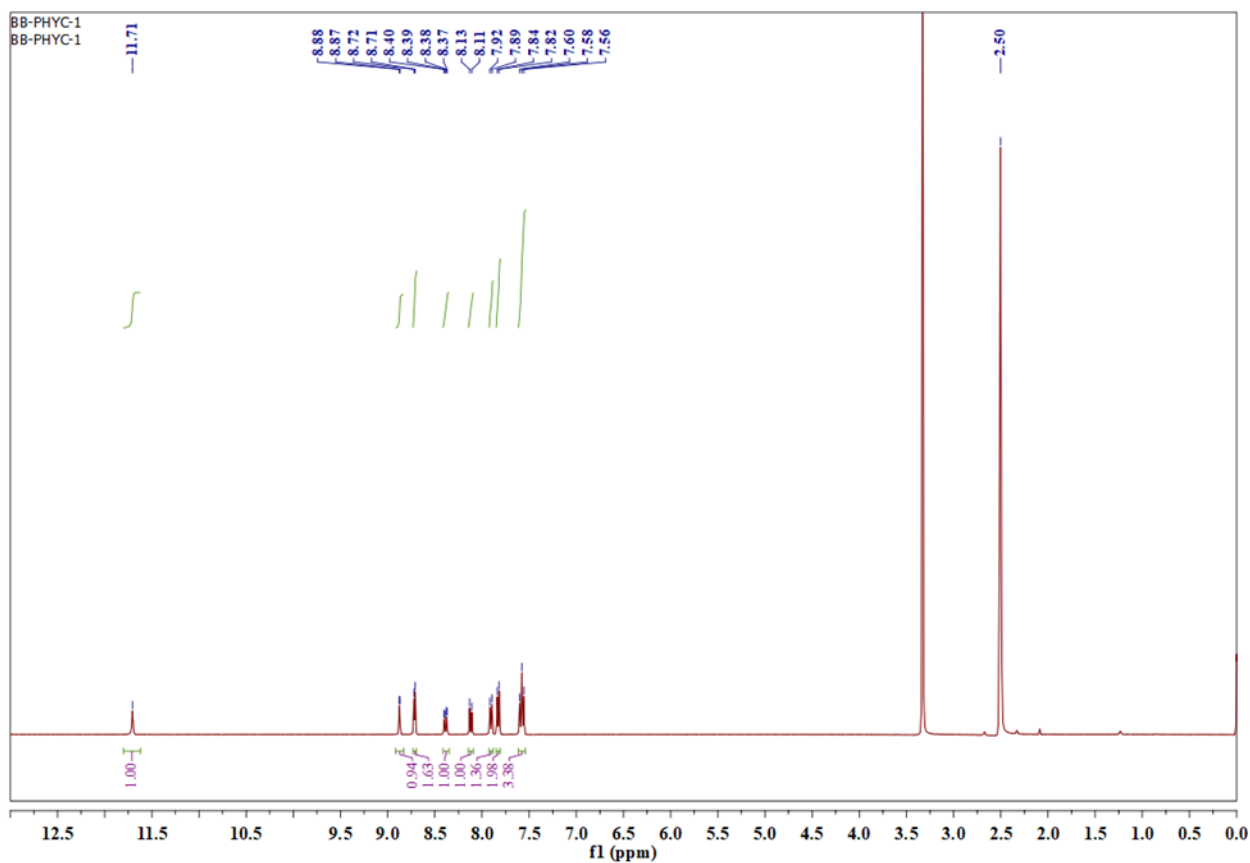


Figure S1. ^1H -NMR spectra of L in DMSO-d₆.

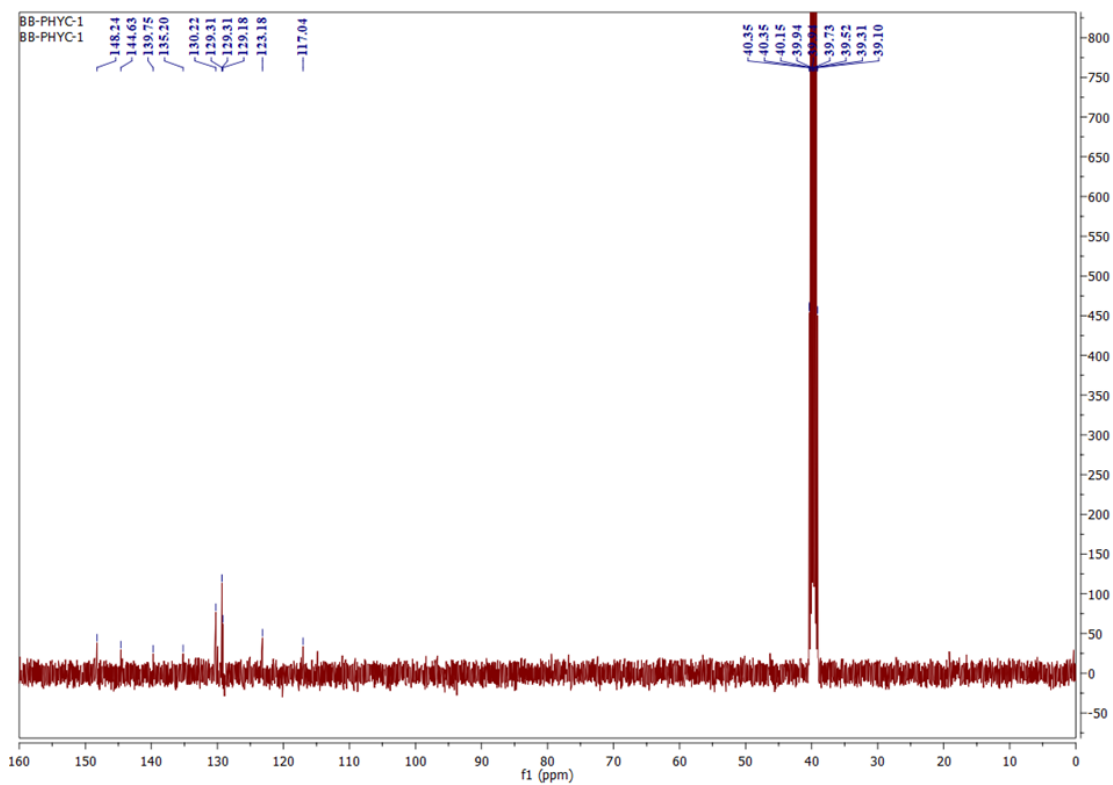


Figure S2. ^{13}C -NMR spectra of L in DMSO-d₆.

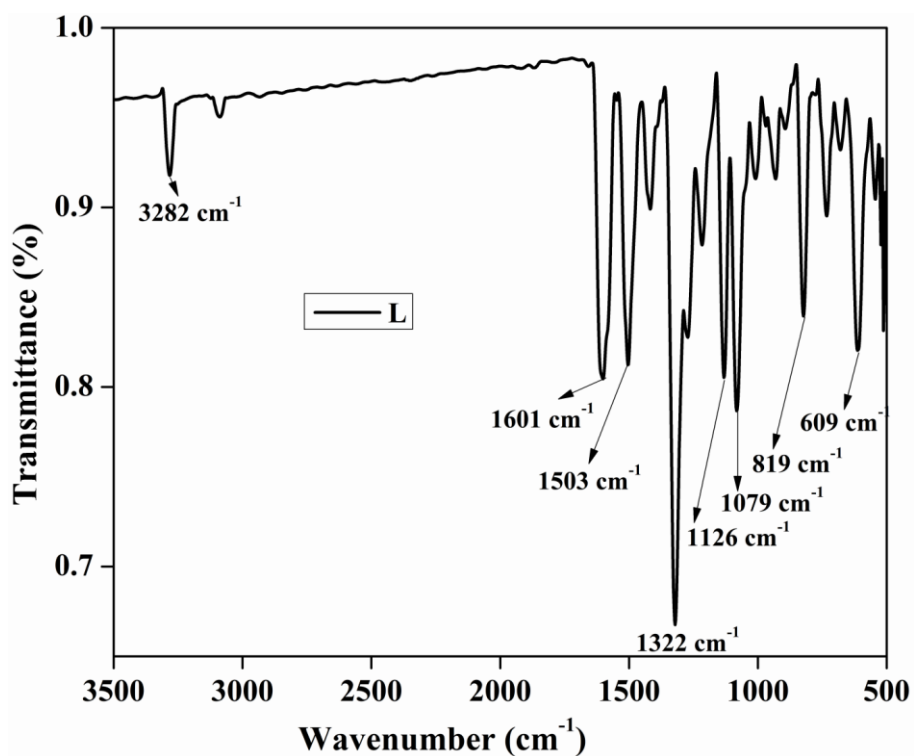


Figure S3. FTIR spectra of L.

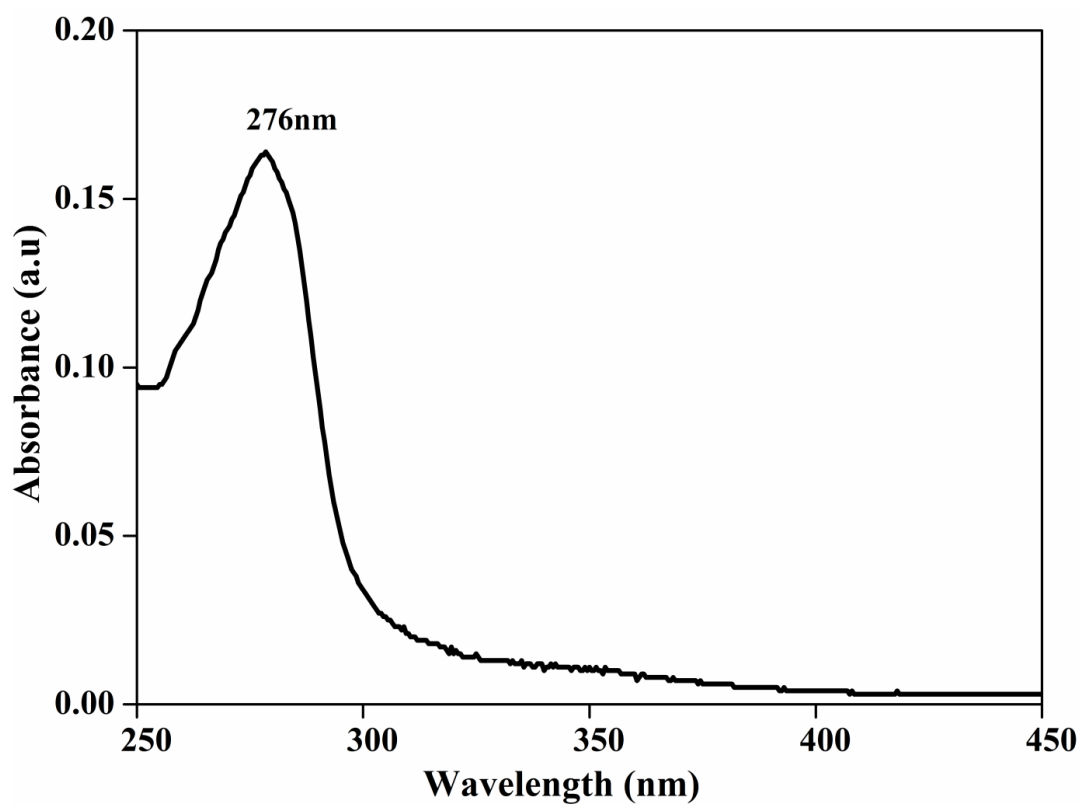


Figure S4. UV-vis spectra of BSA.

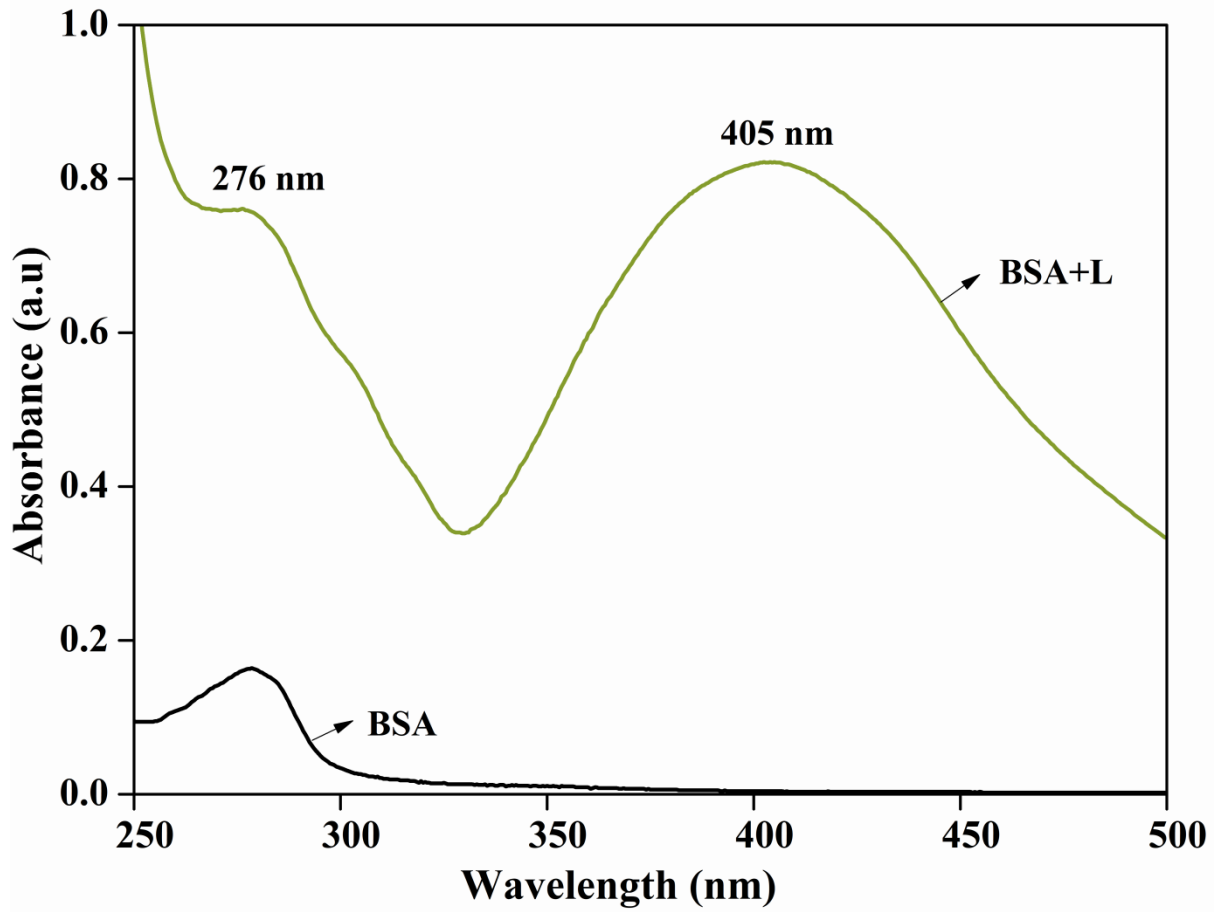


Figure S5. UV-vis spectra of BSA+L.

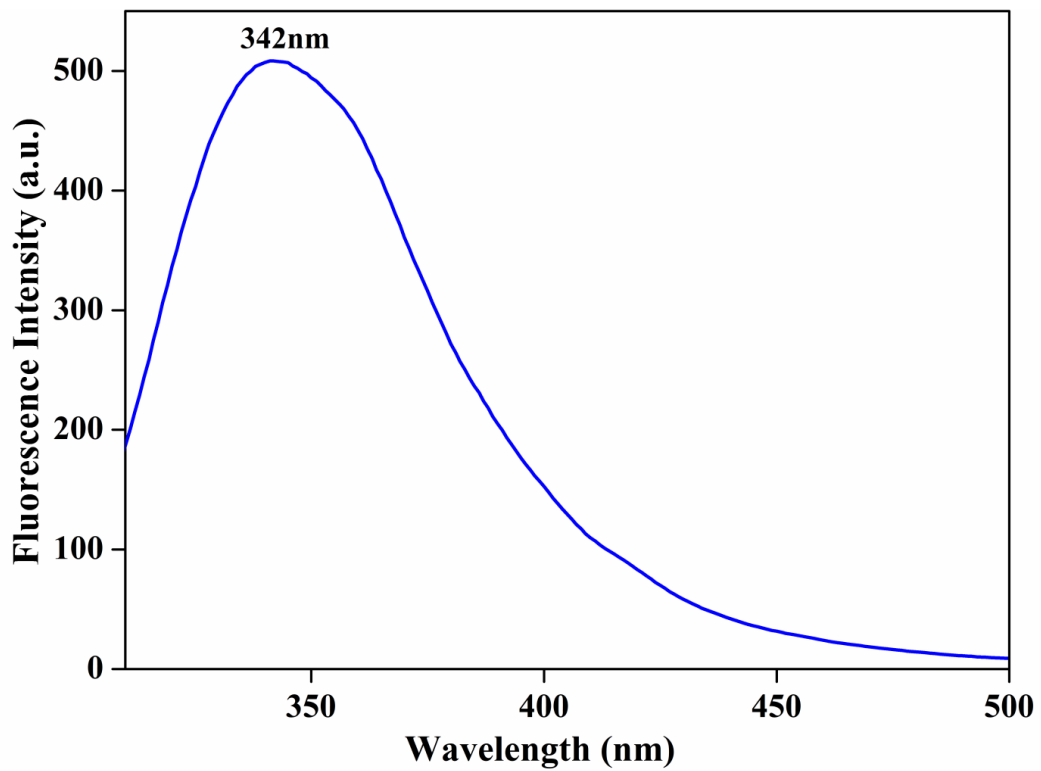


Figure S6. Fluorescence spectra of BSA.

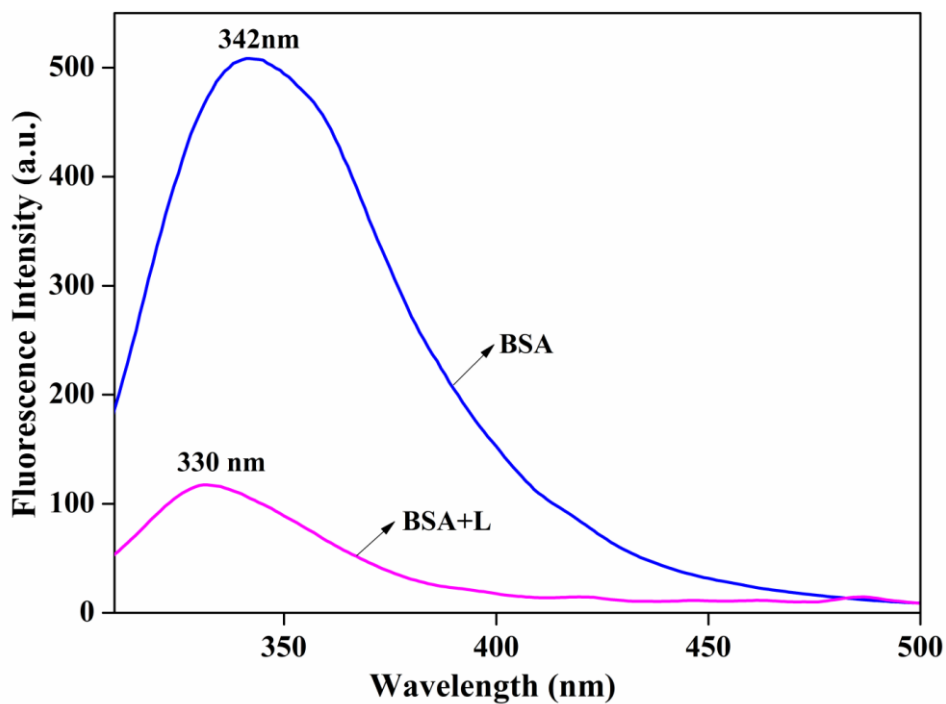


Figure S7. Fluorescence spectra of BSA+L.

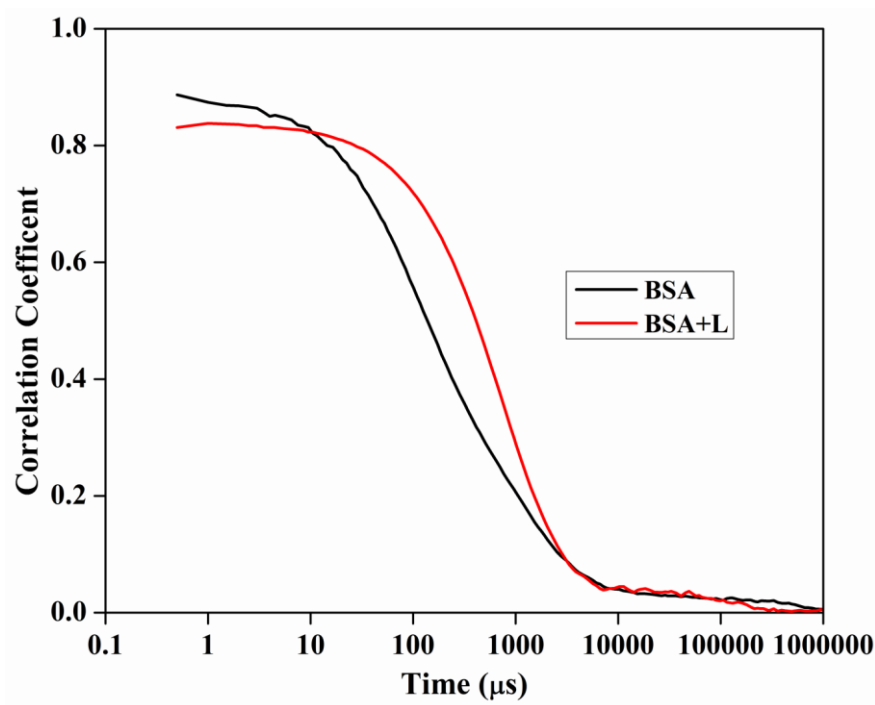


Figure S8. Correlation Coefficient versus time plot for BSA in absence and presence of L.